Published in final edited form as:
Cancer Res. 2014 July 1; 74(13): 3630–3642. doi:10.1158/0008-5472.CAN-13-3615.

Oxidative Stress Activates SIRT2 to Deacetylate and Stimulate Phosphoglycerate Mutase

Yanping Xu[2,3], **Fulong Li**[2,3], **Lei Lv**[1,2], **Tingting Li**[2,3], **Xin Zhou**[2,3], **Chu-Xia Deng**[4], **Kun-Liang Guan**[1,2,5], **Qun-Ying Lei**[1,2], and **Yue Xiong**[1,2,6]

[1]Ministry of Education Key Laboratory of Molecular Medicine, and Department of Biochemistry and Molecular Biology, Shanghai Medical College, Shanghai, PR China [2]Molecular and Cell Biology Lab, Institutes of Biomedical Sciences, Shanghai, PR China [3]School of Life Sciences, Fudan University, Shanghai, PR China [4]Genetics of Development and Disease Branch, National Institute of Diabetes, Digestive and Kidney Diseases, NIH, Bethesda, Maryland [5]Department of Pharmacology and Moores Cancer Center, University of California at San Diego, La Jolla, California [6]Department of Biochemistry and Biophysics, Lineberger Comprehensive Cancer Center, University of North Carolina at Chapel Hill, North Carolina

Abstract

Glycolytic enzyme phosphoglycerate mutase (PGAM) plays an important role in coordinating energy production with generation of reducing power and the biosynthesis of nucleotide precursors and amino acids. Inhibition of PGAM by small RNAi or small molecule attenuates cell proliferation and tumor growth. PGAM activity is commonly upregulated in tumor cells, but how PGAM activity is regulated *in vivo* remains poorly understood. Here we report that PGAM is acetylated at lysine 100 (K100), an active site residue that is invariably conserved from bacteria, to yeast, plant, and mammals. K100 acetylation is detected in fly, mouse, and human cells and in multiple tissues and decreases PGAM2 activity. The cytosolic protein deacetylase sirtuin 2 (SIRT2) deacetylates and activates PGAM2. Increased levels of reactive oxygen species stimulate PGAM2 deacetylation and activity by promoting its interaction with SIRT2. Substitution of endogenous PGAM2 with an acetylation mimetic mutant K100Q reduces cellular NADPH production and inhibits cell proliferation and tumor growth. These results reveal a mechanism of

Corresponding Authors: Yue Xiong, University of North Carolina at Chapel Hill, 22-012 Lineberger Cancer Center, CB# 7295, Chapel Hill, NC 27599. Phone: 919-962-2142; Fax: 919-966-8799; yxiong@email.unc.edu; Kun-Liang Guan, kuguan@ucsd.edu; and Qun-Ying Lei, qlei@fudan.edu.cn.

Disclosure of Potential Conflicts of Interest
No potential conflicts of interest were disclosed.

Note: Supplementary data for this article are available at Cancer Research Online (http://cancerres.aacrjournals.org/).

Authors' Contributions
Conception and design: K.-L. Guan, Q.-Y. Lei, Y. Xiong
Acquisition of data (provided animals, acquired and managed patients, provided facilities, etc.): Y. Xu, L. Lv, T. Li, X. Zhou
Analysis and interpretation of data (e.g., statistical analysis, biostatistics, computational analysis): Y. Xu, K.-L. Guan, Q.-Y. Lei
Writing, review, and or revision of the manuscript: K.-L. Guan, Q.-Y. Lei, Y. Xiong
Administrative, technical, or material support (i.e., reporting or organizing data, constructing databases): F. Li
Study supervision: K.-L. Guan, Q.-Y. Lei, Y. Xiong
Provided key reagents for this study: C.-X. Deng

PGAM2 regulation and NADPH homeostasis in response to oxidative stress that impacts cell proliferation and tumor growth.

Introduction

Enhanced glycolysis, commonly referred to as the “Warburg effect” (1), is a distinctive and prominent feature of cancer cells. One prevalent belief on the benefits of the Warburg effect to tumor cells holds that enhanced glycolysis accumulates glycolytic intermediates, providing substrates for biosynthetic reactions to support cell growth and division. An alternative, but not mutual exclusive, view is that enhanced glycolysis limits the rate of oxidative phosphorylation, thereby helping cells within the tumor to adapt hypoxic condition and protecting them against oxidative damages (2, 3).

Phosphoglycerate mutase (PGAM) is a glycolytic enzyme that catalyzes the reversible conversion of 3-phosphoglycerate (3-PG) to 2-phosphoglycerate (2-PG; ref. 4). Human genome contains two *PGAM* genes, *PGAM1* (also known as *PGAM-B*), which is expressed in brain and most other tissues, and *PGAM2* (also known as *PGAM-M*), which is highly expressed in muscle. Their encoded products are similar in length (254 and 253 residues, respectively), share high degree of homology (81% identity), and form either homo- or heterodimers that are functionally indistinguishable. Both 3-PG and 2-PG are allosteric regulators; 3-PG inhibits 6-phosphogluconate dehydrogenase (6PGD) of pentose phosphate pathway (PPP), whereas 2-PG activates phosphoglycerate dehydrogenase (PHGDH) of glycine and serine synthesis pathway (5). By controlling the levels of its substrate (3-PG) and product (2-PG), PGAM may play a role in coordinating the energy production through glycolysis with generation of reducing power and biosynthesis of amino acids and 5-carbon sugar, the precursors of nucleotides for the synthesis of both RNA and DNA. Supporting a critical role of PGAM activity in cell growth, an unbiased screen for genes that can immortalize mouse embryonic fibroblasts (MEF) identified PGAM2, which when expressed at 2-fold higher level, renders MEFs to indefinite proliferation and resistance to ras-induced senescence (6). Conversely, inhibition of PGAM, by either small RNAi or small molecule, attenuates cell proliferation and tumor growth (5).

The regulation of PGAM is poorly understood. Like other glycolytic enzymes, the activity of PGAM is upregulated in tumor cells, including tumors of lung, colon, liver, breast, and leukemia (5, 7, 8). Most glucose transporter and glycolytic enzymes are transcriptionally regulated by the hypoxia-inducible transcriptional factor HIF-1α (9). Notably, however, of a panel of 18 glucose transporter and glycolytic genes examined, the transcription of 2 genes, *PGAM* and glucose-6-phosphate isomerase (*GPI*), was found not to be induced by HIF-1α (9), suggesting that the activity of these two glycolytic enzymes may be posttranscriptionally regulated. In tumors where an increased PGAM activity has been demonstrated, the steady-state levels of PGAM protein appear to be similar to that of normal tissues compared, suggesting the possibility that the activity of PGAM is subjected to a posttranslational regulation.

Protein acetylation has been recently found as an evolutionarily conserved modification that regulates diverse cellular pathway, including notably the metabolic enzymes (10–15).

Studies on individual enzymes have subsequently demonstrated that acetylation regulates the activity of metabolic enzymes via a variety of different mechanisms (16). In this study, we report that the activity of PGAM is inhibited by lysine acetylation and this mechanism of regulation plays a critical role in oxidative stress response and tumorigenesis.

Materials and Methods

Plasmid construction

Full-length cDNA of PGAM2 was amplified by PCR and cloned into indicated vectors including pRK7-N-FLAG and pQCXIH; SIRT1 and SIRT2 were cloned to pCDNA3-HA vector. Point mutations for PGAM2 were generated by site-directed mutagenesis. The PGAM2 shRNA plasmid (Origene) and the SIRT2 shRNA plasmid (Sigma) were commercially purchased.

Cell culture and transfection

HEK293T and MEF cells were cultured in DMEM (Invitrogen) supplemented with 10% FBS (HyClone), 100 units/mL penicillin, and 100 μg/mL streptomycin (Gibco). Human lung carcinoma A549 cells were cultured in Nutrient Mixture F-12 Ham Kaighn's Modification (F12K) Medium (Sigma) with 10% FBS, 100 units/mL penicillin, and 100 μg/mL streptomycin. Cell transfection was carried out by Lipofectamine 2000 according to the manufacturer's protocol (Invitrogen).

Cell lysis, immunoprecipitation, immunoblotting, and antibody

Cells were lysed in NP-40 buffer containing 50 mmol/L Tris pH 7.5, 150 mmol/L NaCl, 0.3% Nonidet P-40, 1 μg/mL aprotinin, 1 μg/mL leupeptin, 1 μg/mL pepstatin, 1 mmol/L Na_3VO_4, and 1 mmol/L phenylmethylsulfonylfluoride (PMSF). Cell lysates were incubated with anti-Flag beads (Sigma) for 3 hours at 4°C, the beads were washed with NP-40 buffer 3 times and then subjected to SDS-PAGE or eluted by Flag peptides for enzyme activity assay. Western blotting was performed according to standard protocol.

Antibodies specific to Flag (Sigma), HA (Santa Cruz), PGAM2 (Abcam), and β-actin (Sigma) were commercial. Rabbit anti-pan-acetyl lysine antibody and anti-acetyl-PGAM2 K100 antibody (antigen peptide sequence: TGLNKAETAAKH) were generated at Shanghai Genomic Inc.

PGAM2 enzyme activity assay

Purified Flag-PGAM2 protein were incubated with the buffer containing 79 mmol/L triethanolamine, 0.70 mmol/L ADP, 0.15 mmol/L NADH, 6.6 mmol/L 3-phosphoglycerate, 1.3 mmol/L 2,3-diphosphoglycerate, 2.5 mmol/L $MgSO_4$, 99 mmol/L KCl, 4 units pyruvate kinase, 20 units L-lactate dehydrogenase, and 3 units enolase. Activity was measured by the change of absorbance resulting from NADH oxidation in F-4600 Fluorescence Spectrophotometer (HITACHI). All the regents described above were purchased from Sigma.

In vitro deacetylation assay

His-CobB (10 μg/mL) purified from *Escherichia coli* or HA-SIRT1 and HA-SIRT2 purified from HEK293T cells were incubated with Flag-PGAM2 (10 μg/mL) in a HEPES buffer [40 mmol/L HEPES, 1 mmol/L $MgCl_2$, 1 mmol/L dithiothreitol (DTT), 5 mmol/L NAD^+] at 37°C for 1 hour. The effect of CobB deacetylation of PGAM2 was analyzed by Western blotting and measurement of PGAM2 activity.

Preparation of K100-acetylated PGAM2 protein

K100-acetylated PGAM2 was generated by a method described previously (17, 18). Briefly, the clone pTEV8-PGAM2 was constructed to replace the Lys100 with an amber codon that was then co-transformed with pAcKRS-3 and pCDF PylT-1 to BL21. Bacterial cells were grown in LB supplemented with kanamycin (50 mg/mL), spectinomycin (50 mg/mL), and ampicillin (150 mg/mL) and induced with 0.5 mmol/L IPTG, 20 mmol/L nicotinamide (NAM), and 2 mmol/L N^{ε}-acetyl lysine (Sigma) when the concentration of *E. coli* cells reached to OD_{600} of 0.6 (early logarithmic phase). After induction overnight, *E. coli* cells were harvested. Both the wild-type (WT) and K100-acetylated PGAM2 protein were purified by nickel beads for enzyme activity analysis.

Measurement of intracellular reactive oxygen species level

Reactive oxygen species (ROS) production was determined by incubating the A549 stable cells in serum-free medium containing 10 μmol/L fluorescent dye 2′,7′-dichlorofluorescein diacetate (DCF; Sigma) at 37°C for 30 minutes, washing by serum-free medium for three times, followed by fluorescence analysis.

Establishment of knocking-down and putting-back stable cell lines

All retroviruses were produced by co-transfecting the package vector expressing *gag* and *vsvg* genes with the indicated plasmids into HEK293T cells and harvested 48 hours after transfection. A549 cells were transduced with the retrovirus in the presence of 8 μg/mL polybrene. The shRNA plasmid–produced retrovirus-infected cells were selected in puromycin (2 μg/mL) for knocking-down and the pQCXIH plasmid–produced retrovirus-infected cells were selected in hygromycin (350 mg/mL) for putting-back. After 7 to 12 days of selection, the expression levels of PGAM2 were determined by Western blotting.

Cell proliferation and xenograft studies

A total of 5×10^4 indicated stable cells were seeded in triplicate in 6-well plates, and cell numbers were counted every day over a 4-day period. Nude mice (*nu*/*nu*, male, 6- to 7-week-old) were injected subcutaneously with 3×10^6 A549 PGAM2 knocking-down and WT or K100Q-mutant putting-back stable cells. Seven weeks later, the tumors were harvested, and the volume and weight of tumors were measured.

Results

PGAM2 is acetylated at an evolutionarily conserved residue, Lys100

We and others recently discovered that most enzymes in the cellular metabolic pathways are acetylated by large-scale mass spectrometry studies (10, 13, 14). Among these, lysine 100 (K100) was identified as a putative acetylation site in a peptide (HYGGLTGLNKAETAAK, with K100 underlined) that could correspond to either PGAM1 or PGAM2 and is highly conserved during the evolution (Fig. 1A; ref. 10). K100 binds to substrate 3-PG as well as intermediate 2,3-PG (19, 20). Molecular modeling suggests that acetylation at K100, if it occurs, could significantly neutralize the charge on the lysine side chain, likely causing a steric hindrance to the binding with substrate 3-PG and thereby inhibiting PGAM activity (Fig. 1B).

To confirm the acetylation of PGAM, we expressed Flag-PGAM2 in HEK293T cells and then treated cells with trichostatin A (TSA) and NAM, two commonly used deacetylase inhibitors that inhibit histone deacetylase HDAC I and II (21) and the SIRT family deacetylases (22), respectively. We found that PGAM2 was indeed acetylated (Fig. 1C), and its acetylation level was enhanced approximately 2.3-fold after treatment of cells with combined NAM (4 hours) and TSA (16 hours). We then mutated K100 to either arginine (K100R) or glutamine (K100Q) and found that both mutations evidently decreased the overall acetylation level of PGAM2 by 58.7% and 62.5%, respectively (Fig. 1D). K100 mutation did not completely abolish the acetylation of PGAM2, indicating that there might be other acetylated sites in PGAM2. As the mutation of K100 reduced 60% of total acetylation level, we concluded that K100 is the major acetylation site of PGAM2.

To confirm K100 acetylation *in vivo*, we generated an antibody specific to the acetylated K100. We first performed dot blot to characterize the specificity of this antibody and found that the anti-AcPGAM2(K100) antibody preferentially recognized the K100-acetylated peptide, but not the unmodified peptide (Supplementary Fig. S1A). Pre-incubation of the anti-AcPGAM2(K100) antibody with the K100-acetylated antigen peptide, but not the unmodified peptide, abolished the signal (Supplementary Fig. S1B), confirming the specificity of the antibody in recognition of the K100-acetylated PGAM2. Western blotting using this antibody detected strong signal of ectopically expressed WT PGAM2 but only weakly recognized the K100R mutant (Fig. 1E). Endogenous K100-acetylated PGAM2 could be readily detected by this antibody, including A549 adenocarcinomic human alveolar basal epithelial cells and HEK293T human embryonic kidney cells (Supplementary Fig. S1C and Fig. 1F). Knocking down PGAM2 abolished the signals detected by the anti-AcPGAM2(K100) antibody (Supplementary Fig. S1C), and conversely treatment of cells with combined deacetylase inhibitors TSA and NAM increased the signals (Fig. 1F). Taking together, we conclude that PGAM is acetylated *in vivo* at lysine 100.

K100 is evolutionarily conserved in PGAM from bacteria, yeast, plant to mammals (Fig. 1A). To determine whether acetylation of K100 is evolutionarily conserved, we treated human A549 lung cancer cells, MEFs, and *Drosophila* S2 cells with deacetylase inhibitors and determined K100 acetylation of endogenous PGAM (Fig. 1G). This experiment demonstrates that K100-acetylated PGAM is readily detected in mouse and fly cells and that

K100 acetylation is dynamically affected by the deacetylase activity in these cells. Finally, taking the advantage of the anti-AcPGAM(K100) antibody, we demonstrate that PGAM is acetylated at K100 differentially in multiple different tissues, highly acetylated in several tissues such as liver, brain, and kidney, and substantially lower in other tissues such as lung, heart, muscle, and spleen (Fig. 1H). Collectively, these experiments demonstrate that K100 acetylation represents an evolutionary conserved regulation on PGAM.

Acetylation at K100 inhibits PGAM2 enzyme activity

To determine the effect of K100 acetylation on PGAM2 enzyme activity, we immunopurified ectopically expressed Flag-PGAM2 from cells that were either untreated or treated with combination of TSA and NAM and then assayed enzyme activity. We found that the activity of PGAM2 decreased approximately 40% after TSA and NAM treatment (Fig. 2A). When purified PGAM2 was incubated with bacterial deacetylase CobB *in vitro*, the activity of PGAM2 increased by as much as 85% (Fig. 2B). These results indicate that K100 acetylation has an inhibitory effect on PGAM2 activity. To further test this notion, we transfected HEK293T cells with WT, K100R or K100Q mutants PGAM2 and then immunopurified to measure their activity. We found that mutation of Lys100 to Arg substantially reduced the activity of PGAM2, whereas notably the acetylation mimic mutant $PGAM2^{K100Q}$ nearly completely (97%) abolished PGAM2 activity (Fig. 2C). Moreover, treatment of TSA and NAM or incubation with bacterial deacetylase CobB, while significantly affected the activity of WT PGAM2, had little effect on the activity of either $PGAM2^{K100R}$ or $PGAM2^{K100Q}$ mutants (Fig. 2D and E). Taking together, these results indicate that Lys100 is critically important for the activity of PGAM. To determine how K100 acetylation affects PGAM2 activity, we expressed wild-type PGAM2 and acetylation mimetic K100Q mutant in the cells and then did the gel filtration assay and binding assay. We found that K100 acetylation does not affect PGAM dimerization (Supplementary Fig. S3), suggesting that acetylation at K100 could neutralize the charge on the lysine side chain, likely causing a steric hindrance to the binding with substrate 3-PG and thereby inhibiting PGAM activity as the modeling showed (Fig. 1B). We also found that there is an inverse correlation between K100 acetylation and PGAM activity in different mouse tissues. For example, both lungs and muscle have relatively high PGAM enzymatic activity and low K100 acetylation, whereas the brain, liver, and kidneys have relatively low activity and high K100 acetylation level (Fig. 1H and Supplementary Fig. S2). This result is consistent with the notion that the K100 acetylation negatively regulates the activity of PGAM *in vivo*.

To provide definitive evidence that acetylation at K100 inhibits PGAM activity, we used the genetic encoding system that can generate homogeneous acetylated recombinant protein at specific lysine (23, 24). We found that K100-acetylated PGAM2 protein has substantially reduced (by 96%) enzymatic activity when compared with the WT PGAM2 (Fig. 2F). Collectively, these observations supported the conclusion that acetylation at K100 inhibits PGAM2 activity.

SIRT2 is responsible for deacetylation of PGAM2 at K100

Lysine acetylation is a reversible process, which is catalyzed by the acetyl transferases and deacetylases. To identify the deacetylase responsible for PGAM2 K100 acetylation, we

treated HEK293T cells with TSA or NAM separately and found that levels of K100 acetylation were unchanged in HDAC inhibitor TSA-treated cells but were increased in cells treated with SIRT inhibitor NAM (Fig. 3A). Treatment of cells with combination of TSA and NAM did not further increase K100 acetylation appreciably compared with that in cells treated with NAM alone. These results indicate that an NAD^+-dependent sirtuin family deacetylase is likely involved in K100 deacetylation.

Given that PGAM2 is a cytosolic protein, we first determined the interactions between PGAM2 and the 2 cytoplasmic localized SIRTs—SIRT1 and SIRT2 and found that SIRT2, but not SIRT1, binds to PGAM2 (Fig. 3B). Upon expression of SIRT1, SIRT2, and the SIRT2 catalytic inactive mutant H187Y in HEK293T cells, only the WT SIRT2 could decrease the levels of K100 acetylation of both exogenously and endogenously expressed PGAM (Fig. 3C and Supplementary Fig. S4), supporting that SIRT2 is a deacetylase for PGAM2. To further strengthen this finding, we treated cells with SIRT2-specific inhibitor, salermide (17), and found that salermide treatment increased the K100 acetylation level in a dose-dependent manner (Fig. 3D). Similarly, knocking down *SIRT2* significantly increased K100 acetylation (Fig. 3E). Moreover, *Sirt2* knockout (KO) MEFs have higher acetylation levels at K100 of PGAM than WT MEFs. Putting-back of human SIRT2 partially restored K100 acetylation of PGAM (Fig. 3F). The K100 acetylation level is conversely correlated with the SIRT2 protein level. Taken together, these results demonstrated that SIRT2 is the main deacetylase that acts on PGAM K100 deacetylation.

SIRT2 regulates PGAM2 activity via K100 acetylation

Because K100 acetylation inhibits PGAM activity, SIRT2 may therefore act as a positive regulator of PGAM. To test this possibility, we examined the role of SIRT2 in regulation of PGAM2 enzyme activity. First, we immunopurified ectopically expressed Flag-PGAM2 from HEK293T cells treated with deacetylase inhibitors and measured the activity. Consistent with the suggestion that SIRT2 stimulates PGAM2 activity, treatment of cells with NAM, but not TSA, decreased the activity of PGAM2 (Supplementary Fig. S5). Next, we co-expressed PGAM2 with either SIRT1 or SIRT2 in HEK293T cells and found that SIRT2, but not SIRT1, decreased K100 acetylation and increased the activity of PGAM2 approximately by 60% (Fig. 4A). Conversely, knocking down SIRT2 or inhibiting SIRT2 with salermide reduced PGAM2 activity (Fig. 4B and C). Together, these data show that SIRT2 activates PGAM2 activity.

SIRT2 co-expression, however, had little effect on the activity of $PGAM2^{K100R}$ and $PGAM2^{K100Q}$ mutants (Fig. 4D), suggesting that SIRT2 activates PGAM2 mostly via deacetylating K100. To further support this notion, we carried out *in vitro* deacetylation assay and then measured PGAM2 activity. We found that SIRT2, but not SIRT1, deacetylated and activated PGAM2 in an NAD^+-dependent manner (Fig. 4E), providing a direct evidence supporting SIRT2 in PGAM2 activation.

Oxidative stress induces PGAM2 activity through decreasing K100 acetylation levels

Ectopic overexpression of PGAM2 has been reported to cause immortalization of MEFs, and this process is attributed to the reduced ROS production that protects cells from

oxidative damage (6). To determine whether the K100 acetylation of PGAM is regulated *in vivo*, we treated cells with hydrogen peroxide (H_2O_2) to induce oxidative stress and examined PGAM acetylation and enzymatic activity. We observed that endogenous levels of K100 acetylation were decreased in a time-dependent manner in both HEK239T and A549 cells (Fig. 5A). We immunopurified ectopically expressed Flag-PGAM2 from H_2O_2 treated cells and found that along with a reduction of K100 acetylation, PGAM2 activity was increased more than 2-fold upon H_2O_2 treatment (Fig. 5B). Moreover, H_2O_2 treatment had no significant effect on the activity of $PGAM2^{K100Q}$ and $PGAM2^{K100R}$ mutants (Fig. 5C), indicating that oxidative stress enhanced PGAM2 activity via K100 deacetylation. To determine whether the endogenous PGAM activity is regulated by oxidative stress, we treated HEK293T and MEF cells with H_2O_2 or another oxidative stressor, menadione, a polycyclic aromatic ketone that generates intracellular ROS at multiple cellular sites through futile redox cycling. We found that either H_2O_2 or menadione treatments reduced K100 acetylation of endogenous PGAM, which is associated with an increase of PGAM activity (Fig. 5D). We therefore conclude that oxidative stress enhanced PGAM activity via reducing K100 acetylation.

To elucidate how K100 acetylation was changed in response to oxidative stress, we determined the interaction of PGAM2 and SIRT2 in the cells after H_2O_2 treatment. Immunoprecipitation and Western blot analyses demonstrated that increased oxidative stress promoted the SIRT2 binding to PGAM2 (Fig. 5E). Notably, H_2O_2 treatment did not affect K100 acetylation in *Sirt2* knocking-out MEFs but decreased K100 acetylation after putting back human *SIRT2* in $Sirt2^{-/-}$ MEFs (Fig. 5F). These results demonstrate that the oxidative stress–induced reduction of PGAM2 K100 acetylation is SIRT2-dependent.

Acetylation mimetic K100Q mutant reduces NADPH and impairs oxidative stress response

3-PG and 2-PG are the substrate and product of phosphoglycerate mutase, respectively, and are two important metabolites in cell metabolism. 3-PG can bind to and inhibit the activity of 6PGD, which is a critical enzyme for NADPH production in the PPP and functions to protect cells from oxidative damage (5). To explore the physiologic significance of acetylation in the regulation of PGAM, we established stable cell lines in A549 cells with knocking down of endogenous PGAM2 and putting back of Flag-tagged WT or K100Q mutant of PGAM2, respectively (Fig. 6A), followed by the measurement of NADPH. We found that the NADPH level decreased 48% in A549 cells expressing $PGAM2^{K100Q}$ compared with cells expressing WT PGAM2 (Fig. 6B). This data indicates that acetylation-mimetic mutation at Lys100 impaired the function of PGAM2 in NADPH production, possibly by accumulating its substrate, 3-PG, and thereby increasing the inhibitory effect toward 6PGD. We also compared ROS levels in these two cell lines by DCF, a chemically reduced form of fluorescein that upon cleavage of the acetate groups by intracellular esterase and oxidation can be used as an indicator for ROS in cells. Consistent with the notion that acetylation mimetic K100Q mutant impaired the function of PGAM2 in NADPH production, the A549 cells expressing $PGAM2^{K100Q}$ mutant showed 73% increased DCF staining (Fig. 6C). Supporting the functional importance of K100 acetylation in regulating cellular response to oxidative response, A549 cells expressing $PGAM2^{K100Q}$ mutant were much more sensitive to H_2O_2 than that cell expressing WT PGAM2 (Fig. 6D). Collectively,

the above data show that acetylation at K100 of PGAM2 impaired the ability of cells to respond to oxidative stress.

As SIRT2 catalyzes K100 deacetylation of PGAM2, next we examined the oxidative stress response of both *sirt2* KO MEFs. We found that *sirt2* KO MEFs are more sensitive to oxidative stress than human *SIRT2* putting-back MEFs (Fig. 6E). To test whether this observation is due to PGAM2 K100 acetylation, we overexpressed WT or K100Q-mutant PGAM2 in *sirt2* KO MEFs and found that cells overexpressing WT PGAM2, but not cells overexpressing K100Q mutant, could partially rescue the viability of *sirt2* KO MEF cells after oxidative stress (Fig. 6F). These results demonstrate that the sensitivity of *sirt2* KO MEFs to oxidative stress is, at least partially, due to PGAM2 K100 acetylation.

Acetylation mimetic K100Q mutant suppressed cell proliferation and tumor growth

Given the high activity of phosphoglycerate mutase in cancer cells, we examined the effect of K100 acetylation of PGAM2 on cell proliferation and tumor growth. We found that A549 cells that knocked down endogenous PGAM2 and ectopically expressed acetylation-mimetic $PGAM2^{K100Q}$ proliferated significantly slower than cells expressing WT PGAM2, indicating that acetylation of K100 regulates cell growth (Fig. 7A). To further determine whether K100 acetylation of PGAM2 plays a critical role in tumor growth, we performed xenograft assay in immunodeficient nude mice using the A549 stable cell lines described above. Three million cells with putting-back of either WT or K100Q-mutant PGAM2 were injected into nude mice subcutaneously, and tumors were dissected after around 7 weeks. The expression levels of putting-back Flag-tagged WT PGAM2 and K100Q mutant in xenograft tumors were verified by Western blot analysis (Fig. 7B). We found that cells expressing $PGAM2^{K100Q}$ developed tumors much slower than cells expressing WT PGAM2, as determined by both tumor volume (Fig. 7C and D) and tumor weight (Fig. 7E). Taken together, these results demonstrate that PGAM2 K100 acetylation inhibits tumor cell growth *in vivo*.

Discussion

In this article, we provide 4 lines of evidence to demonstrate that acetylation plays a critical role in the regulation of PGAM enzyme activity. First, K100, a highly conserved residue in PGAM, is acetylated *in vivo* in multiple tissues and K100 acetylation is an evolutionarily conserved modification from fly to mammals. Second, K100 acetylation inhibits the activity of PGAM. Third, SIRT2 directly binds to and deacetylates PGAM, leading to its activation and, importantly, oxidative stress promotes SIRT2-PGAM binding, induces deacetylation at K100, and activates PGAM activity. Finally, replacement of endogenous PGAM with an acetylation mimetic mutant, like the inhibition of PGAM by RNAi-mediated depletion or pharmacologic inhibitor, suppresses cell proliferation and tumor growth.

PGAM catalyzes the 3-PG-to-2-PG isomerization via a 2-step process, as opposed to a direct transfer of a phosphate; first, a transfer of phosphate group from phosphohistidine (H11 in human PGAM) in the active site to the C-2 carbon of 3-PG to form 2,3-bisphosglycerate (2,3-PG) and then the transfer of the phosphate group linked on C-3 carbon of 2,3-PG to the catalytic histidine, resulting in the regeneration of phosphohistidine and the release of

product, 2-PG. Because of this prominent enzyme substitution catalytic feature and its critical role in metabolic pathway, PGAM has been the subject of extensive investigation by X-ray crystallography. These studies have demonstrated a highly conserved structure of PGAM, in particular the active site (18–20). Lys100 is a key residue of the active site and contacts directly with both the substrate, 3PG, and the intermediate, 2,3-PG (25). As acetylation would neutralize the positive charge of the lysine side chain, a likely molecular basis for the inhibition of PGAM activity by K100 acetylation is that covalent linkage of the acetyl group on K100 interferes with the binding of PGAM with both the substrate and the intermediate. An alternative possibility is that acetylation of K100, which is close to the His11, could conceivably affect either the phosphorylation of the catalytic histidine or the transfer of phosphate group to the substrate.

Increased expression of PGAM, by a mere of 2-fold, results in MEF immortalization and, conversely, inhibition of PGAM, by either small RNAi or small molecule, attenuates cell proliferation and tumor growth (5, 6). Supporting the role of PGAM in limiting cell proliferation, we show in this study that replacement of endogenous of PGAM with an acetylation-mimetic K100Q mutant results in significant decrease in cell proliferation and tumor growth in a nude mice xenograft tumor model. Our study further links the regulation of PGAM activity to cellular response to oxidative stress. This is evidenced by the findings that oxidative stress increases the PGAM-SIRT2 binding, leading to a decrease of K100 acetylation and enhanced PGAM enzyme activity. Cellular response to oxidative stress, including angiogenesis and tumorigenesis, is mediated by the HIF-1α (26, 27), which is required for the upregulation of mRNAs encoding glucose transporters and glycolytic enzymes, with notably exception of PGAM (9). Our study, therefore, not only reveals a previously unrecognized regulatory mechanism on PGAM via a posttranslational modification but also a distinctive regulation of PGAM that would allow cells to coordinatively regulate glycolytic pathway genes for metabolic adaptation.

Supplementary Material

Refer to Web version on PubMed Central for supplementary material.

Acknowledgments

The authors thank the members of the Fudan Molecular and Cell Biology laboratory for discussions throughout this study. They also thank Brenda Temple of R.L. Juliano Structural Bioinformatics Core facility at the University of North Carolina at Chapel Hill for the molecular modeling.

Grant Support

This work was supported by 973 (grant no. 2011CB910600, 2009CB918401), NSFC (grant no. 31071192, 81225016), Shanghai Key Basic Research Program (12JC1401100), “100 Talents” Program of Shanghai Health (grant no. XBR2011041), Scholar of “Dawn” Program of Shanghai Education Commission, and Shanghai Outstanding Academic Leader (grant no. 13XD1400600) to Q.-Y. Lei. This work was also supported by the 985 Program, the Shanghai Leading Academic Discipline Project (project number B110), Biomedical Core Facility, Fudan University; Fudan University Interdisciplinary Research Program of outstanding Ph.D. students Funds (Y. Xu), and NIH grants (Y. Xiong and K.-L. Guan).

References

1. Warburg O. On the origin of cancer cells. Science. 1956; 123:309–14. [PubMed: 13298683]

2. Kroemer G, Pouyssegur J. Tumor cell metabolism: cancer's Achilles' heel. Cancer Cell. 2008; 13:472–82. [PubMed: 18538731]

3. Vander Heiden MG, Cantley LC, Thompson CB. Understanding the Warburg effect: the metabolic requirements of cell proliferation. Science. 2009; 324:1029–33. [PubMed: 19460998]

4. Fothergill-Gilmore LA, Watson HC. The phosphoglycerate mutases. Adv Enzymol Relat Areas Mol Biol. 1989; 62:227–313. [PubMed: 2543188]

5. Hitosugi T, Zhou L, Elf S, Fan J, Kang HB, Seo JH, et al. Phosphoglycerate mutase 1 coordinates glycolysis and biosynthesis to promote tumor growth. Cancer Cell. 2012; 22:585–600. [PubMed: 23153533]

6. Kondoh H, Lleonart ME, Gil J, Wang J, Degan P, Peters G, et al. Glycolytic enzymes can modulate cellular life span. Cancer Res. 2005; 65:177–85. [PubMed: 15665293]

7. Durany N, Joseph J, Campo E, Molina R, Carreras J. Phosphoglycerate mutase, 2,3-bisphosphoglycerate phosphatase and enolase activity and isoenzymes in lung, colon and liver carcinomas. Br J Cancer. 1997; 75:969–77. [PubMed: 9083331]

8. Durany N, Joseph J, Jimenez OM, Climent F, Fernandez PL, Rivera F, et al. Phosphoglycerate mutase, 2,3-bisphosphoglycerate phosphatase, creatine kinase and enolase activity and isoenzymes in breast carcinoma. Br J Cancer. 2000; 82:20–7. [PubMed: 10638961]

9. Iyer NV, Kotch LE, Agani F, Leung SW, Laughner E, Wenger RH, et al. Cellular and developmental control of O2 homeostasis by hypoxia-inducible factor 1 alpha. Genes Dev. 1998; 12:149–62. [PubMed: 9436976]

10. Choudhary C, Kumar C, Gnad F, Nielsen ML, Rehman M, Walther T, et al. Lysine acetylation targets protein complexes and co-regulates major cellular functions. Science. 2009; 325:834–40. [PubMed: 19608861]

11. Weinert BT, Scholz C, Wagner SA, Iesmantavicius V, Su D, Daniel JA, et al. Lysine succinylation is a frequently occurring modification in prokaryotes and eukaryotes and extensively overlaps with acetylation. Cell Rep. 2013; 4:842–51. [PubMed: 23954790]

12. Weinert BT, Wagner SA, Horn H, Henriksen P, Liu WR, Olsen JV, et al. Proteome-wide mapping of the Drosophila acetylome demonstrates a high degree of conservation of lysine acetylation. Sci Signal. 2011; 4:ra48. [PubMed: 21791702]

13. Zhao S, Xu W, Jiang W, Yu W, Lin Y, Zhang T, et al. Regulation of cellular metabolism by protein lysine acetylation. Science. 2010; 327:1000–4. [PubMed: 20167786]

14. Kim SC, Sprung R, Chen Y, Xu Y, Ball H, Pei J, et al. Substrate and functional diversity of lysine acetylation revealed by a proteomics survey. Mol Cell. 2006; 23:607–18. [PubMed: 16916647]

15. Wang Q, Zhang Y, Yang C, Xiong H, Lin Y, Yao J, et al. Acetylation of metabolic enzymes coordinates carbon source utilization and metabolic flux. Science. 2010; 327:1004–7. [PubMed: 20167787]

16. Xiong Y, Guan KL. Mechanistic insights into the regulation of metabolic enzymes by acetylation. J Cell Biol. 2012; 198:155–64. [PubMed: 22826120]

17. Lara E, Mai A, Calvanese V, Altucci L, Lopez-Nieva P, Martinez-Chantar ML, et al. Salermide, a Sirtuin inhibitor with a strong cancer-specific proapoptotic effect. Oncogene. 2009; 28:781–91. [PubMed: 19060927]

18. Campbell JW, Watson HC, Hodgson GI. Structure of yeast phosphoglycerate mutase. Nature. 1974; 250:301–3. [PubMed: 4605155]

19. Rigden DJ, Alexeev D, Phillips SE, Fothergill-Gilmore LA. The 2.3 A X-ray crystal structure of *S. cerevisiae* phosphoglycerate mutase. J Mol Biol. 1998; 276:449–59. [PubMed: 9512715]

20. Wang Y, Wei Z, Liu L, Cheng Z, Lin Y, Ji F, et al. Crystal structure of human B-type phosphoglycerate mutase bound with citrate. Biochem Biophys Res Commun. 2005; 331:1207–15. [PubMed: 15883004]

21. Ekwall K, Olsson T, Turner BM, Cranston G, Allshire RC. Transient inhibition of histone deacetylation alters the structural and functional imprint at fission yeast centromeres. Cell. 1997; 91:1021–32. [PubMed: 9428524]

22. Avalos JL, Bever KM, Wolberger C. Mechanism of sirtuin inhibition by nicotinamide: altering the NAD(+) cosubstrate specificity of a Sir2 enzyme. Mol Cell. 2005; 17:855–68. [PubMed: 15780941]

23. Neumann H, Hancock SM, Buning R, Routh A, Chapman L, Somers J, et al. A method for genetically installing site-specific acetylation in recombinant histones defines the effects of H3 K56 acetylation. Mol Cell. 2009; 36:153–63. [PubMed: 19818718]

24. Neumann H, Peak-Chew SY, Chin JW. Genetically encoding N(epsilon)-acetyllysine in recombinant proteins. Nat Chem Biol. 2008; 4:232–4. [PubMed: 18278036]

25. Davies DR, Staker BL, Abendroth JA, Edwards TE, Hartley R, Leonard J, et al. An ensemble of structures of *Burkholderia pseudomallei* 2,3-bisphosphoglycerate-dependent phosphoglycerate mutase. Acta Crystallogr Sect F Struct Biol Cryst Commun. 2011; 67:1044–50.

26. Gao P, Zhang H, Dinavahi R, Li F, Xiang Y, Raman V, et al. HIF-dependent antitumorigenic effect of antioxidants *in vivo*. Cancer Cell. 2007; 12:230–8. [PubMed: 17785204]

27. Shi DY, Xie FZ, Zhai C, Stern JS, Liu Y, Liu SL. The role of cellular oxidative stress in regulating glycolysis energy metabolism in hepatoma cells. Mol Cancer. 2009; 8:32. [PubMed: 19497135]

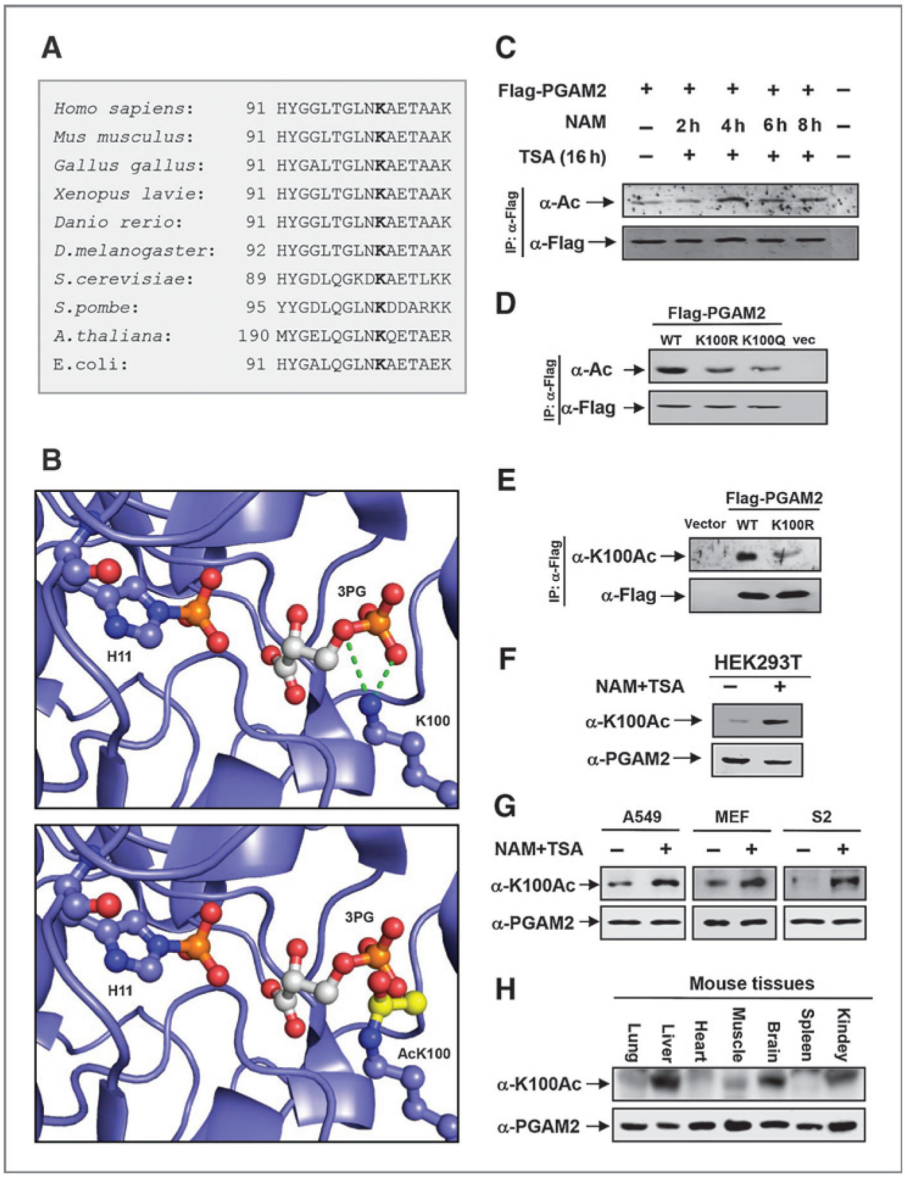

Figure 1.

PGAM2 is acetylated at K100. A, sequence alignment of PGAM surrounding K100 from various species, including human (*Homo sapiens*, NCBI reference number: NP_002620.1), mouse (*Mus musculus*, NP_0075907), chicken (*Gallus gallus*, NP_001026727), frog (*Xenopus laevis*, NP_001084996), zebrafish (*Danio rerio*, NP_942099.1), fruitfly (*Drosophila melanogaster*, AAF56866.2), thale cress (*Arabidopsis thaliana*, O04499), budding yeast (*Saccharomyces cerevisiae*, P00950), fission yeast (*Schizosaccharomyces pombe*, P36623), and bacterial (*E. coli*, WP_001333397.1). Bold, lysine 100. B, molecular modeling of acetylation of K100 in PGAM. The 3-PG binding site of PGAM (from *Burkholderia pseudomallei*, which shares 60% sequence identity with human PGAM) is rendered in the slate blue cartoon. The phosphorylated H11 is shown in slate blue (carbon), blue (nitrogen), red (oxygen), and orange (phosphorus). 3-PG is shown in sticks with carbon

atoms colored white, oxygen atoms colored red, and phosphorus atoms colored orange. The green dashed lines represent critical electrostatic interactions between the lysine side chain and the oxygen of the phosphate of 3-PG. The acetyl group is colored in yellow (carbons). C, PGAM2 is acetylated. Flag-PGAM2 was transfected into HEK293T cells followed by treatment with TSA and NAM for indicated time. PGAM2 acetylation and protein levels were analyzed by Western blotting with indicated antibody. D, K100 is the primary acetylation site of PGAM2. The indicated plasmids were transfected into HEK293T cells and proteins were immunoprecipitated, followed by Western blot for acetylation analyses. E, the plasmids were transfected into HEK293T cells; acetylation levels of immunoprecipitated Flag-PGAM2 and K100R mutant were probed with the site-specific K100 acetylation antibody (α-K100Ac). F, endogenous PGAM2 is acetylated at K100. The HEK293T cells lysate were prepared after TSA and NAM treatment. Endogenous PGAM2 protein and K100 acetylation levels were determined by Western blotting with indicated antibodies. G, K100 acetylation is evolutionarily conserved. The A549, MEF, and S2 cells lysate were prepared after TSA and NAM treatment, respectively. Endogenous PGAM2 protein and K100 acetylation levels were determined by Western blotting with indicated antibodies. H, K100 acetylation is broadly distributed in different tissues. The indicated tissues were isolated from C57BL6 mouse and the lysate was prepared after homogenized. Endogenous PGAM2 protein and K100 acetylation levels were determined by Western blotting with indicated antibodies. IP, immunoprecipitation.

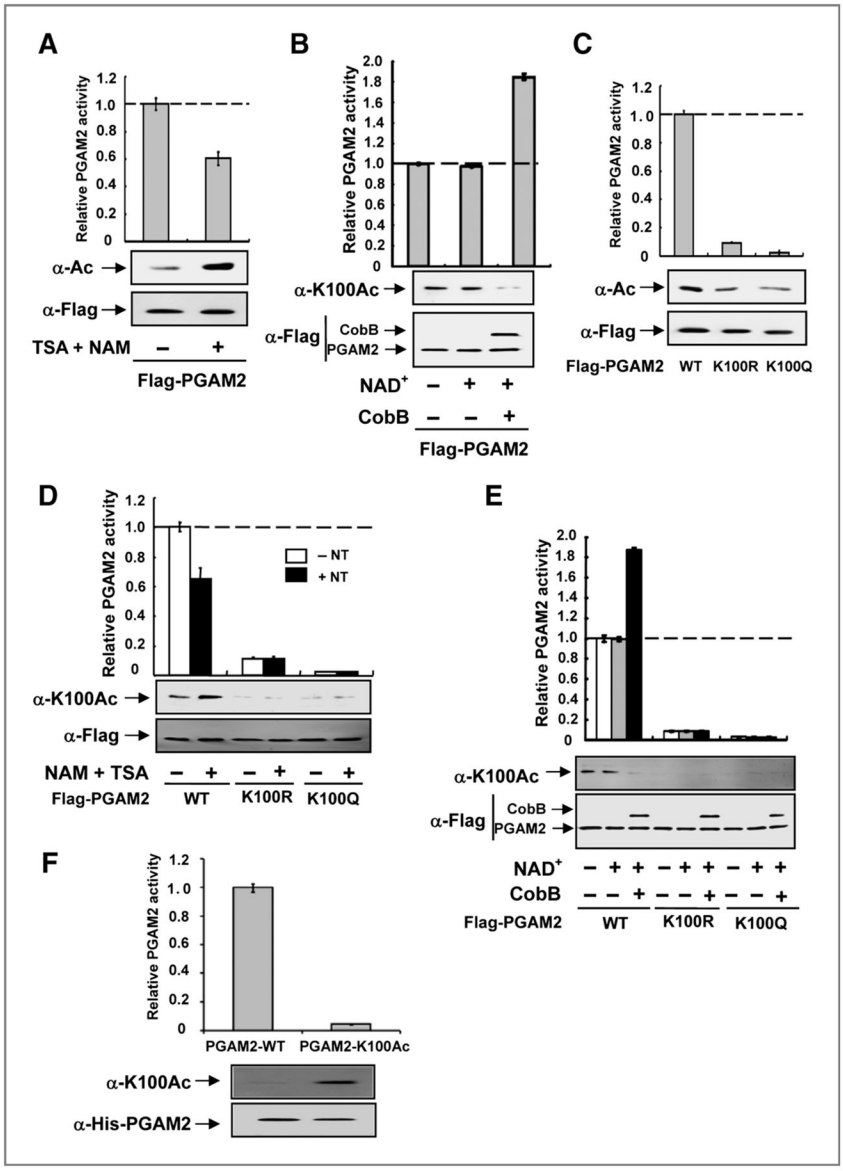

Figure 2.

Acetylation at K100 reduces PGAM2 activity. A, inhibition of deacetylases decreases PGAM2 enzyme activity. Flag-tagged PGAM2 was expressed in HEK293T cells, which were treated with or without TSA and NAM, followed by immunoprecipitation, and enzyme activity was measured and normalized against protein levels. The protein levels and acetylation levels were determined by Western blotting. Mean values ± SD of relative enzyme activity of triplicate experiments are presented. B, PGAM2 is activated by *in vitro* deacetylation. Flag-PGAM2 was expressed in HEK293T cells, purified, and incubated with recombinant CobB. Samples were analyzed for acetylation levels and PGAM2 enzyme activity. Relative enzyme activities of triplicate experiments ± SD are presented. C, K100 mutation decreases PKM2 enzyme activity. Flag-tagged WT and mutant PGAM2 proteins were expressed in HEK293T cells and purified by immunoprecipitation. The enzyme activity was measured and normalized against protein level. Error bars represent ± SD for

triplicate experiments. D, inhibition of deacetylases with TSA and NAM treatment decreases the activity of WT, but not K100-mutant PGAM2. Flag-tagged WT and mutant PGAM2 proteins were expressed in HEK293T cells, followed by treatment with TSA and NAM, and then purified by immunoprecipitation. The PGAM2 enzyme activity was measured and normalized against protein level. The mean value of triplicates and ± SD are presented. E, WT PGAM2, but not K100-mutant PGAM2, is activated by *in vitro* deacetylation. Flag-tagged WT and mutant PGAM2 proteins were expressed in HEK293T cells, then purified and incubated with recombinant CobB, followed by enzyme activity assay. Relative enzyme activities of triplicate experiments ± SD are presented. F, K100-acetylated PGAM2 has lower enzyme activity. Recombinant WT and K100-acetylated PGAM2 protein were purified in *E. coli*. The enzyme activity was measured and normalized against protein level. Mean values of relative enzyme activity of triplicate experiments with ± SD are presented.

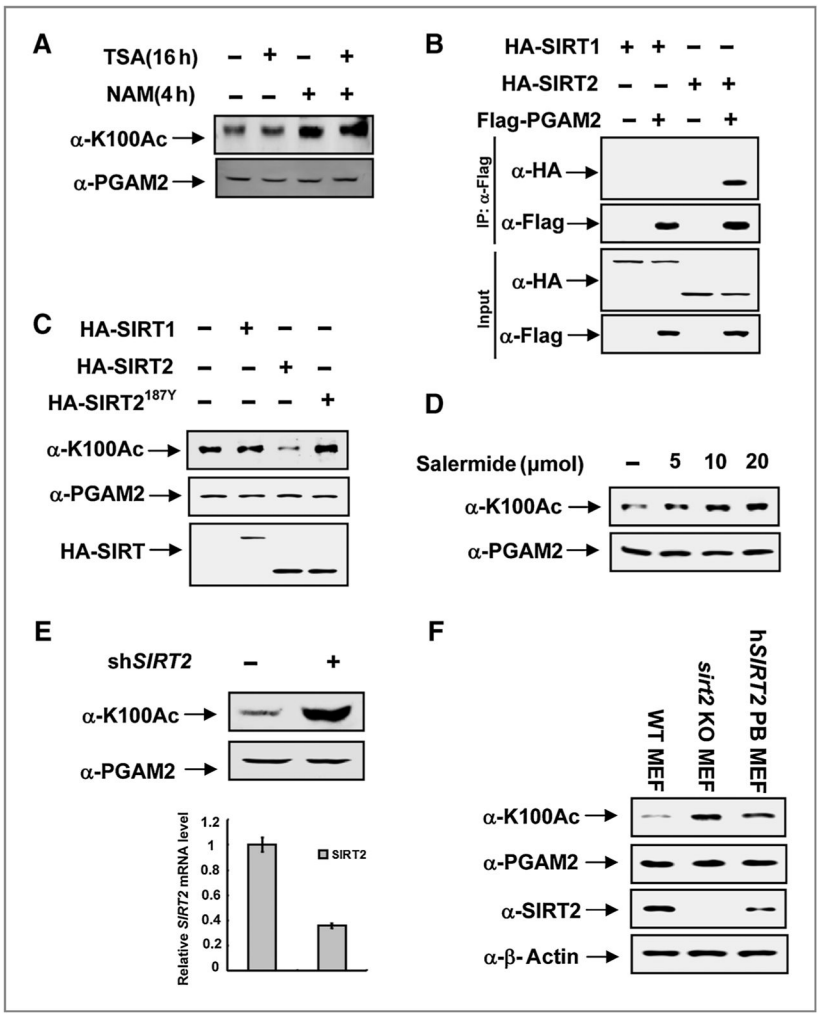

Figure 3.

SIRT2 deacetylates PGAM2 at K100. A, NAM, but not TSA, increases PGAM2 K100 acetylation. HEK293T cells were treated with either NAM or TSA, endogenous PGAM2 protein and K100 acetylation levels were determined by Western blotting with PGAM2 antibody or anti-acetyl-K100 antibody, respectively. B, SIRT2 interacts with PGAM2. HEK293T cells were transfected with indicated plasmids, and interactions between PGAM2 and SIRT1 or SIRT2 were examined by immunoprecipitation and Western blot analysis. C, WT SIRT2 overexpression decreases PGAM2 K100 acetylation. K100 acetylation levels of PGAM2 in HEK293T cells expressing indicated plasmids were detected by Western blotting. D, salermide, the SIRT2 inhibitor, increases the K100 acetylation of PGAM2. HEK293T cells were cultured at different concentrations of salermide. The K100 acetylation levels were probed by anti-acetyl-K100 antibody. E, knocking down SIRT2 increases endogenous K100 acetylation of PGAM2. HEK293T cells were infected with retrovirus targeting SIRT2, and the levels of PGAM2 protein and K100 acetylation were determined by Western blotting. SIRT2 knockdown efficiency was determined by quantitative PCR. Error bars represent ± SD for triplicate experiments. F, the K100 acetylation level of PGAM2 is increased in *sirt2* knockout MEFs and decreased in h*SIRT2* putting-back MEFs.

The indicated cell lysates were prepared, and levels of PGAM2 protein and K100 acetylation were detected by Western blotting using indicated antibodies.

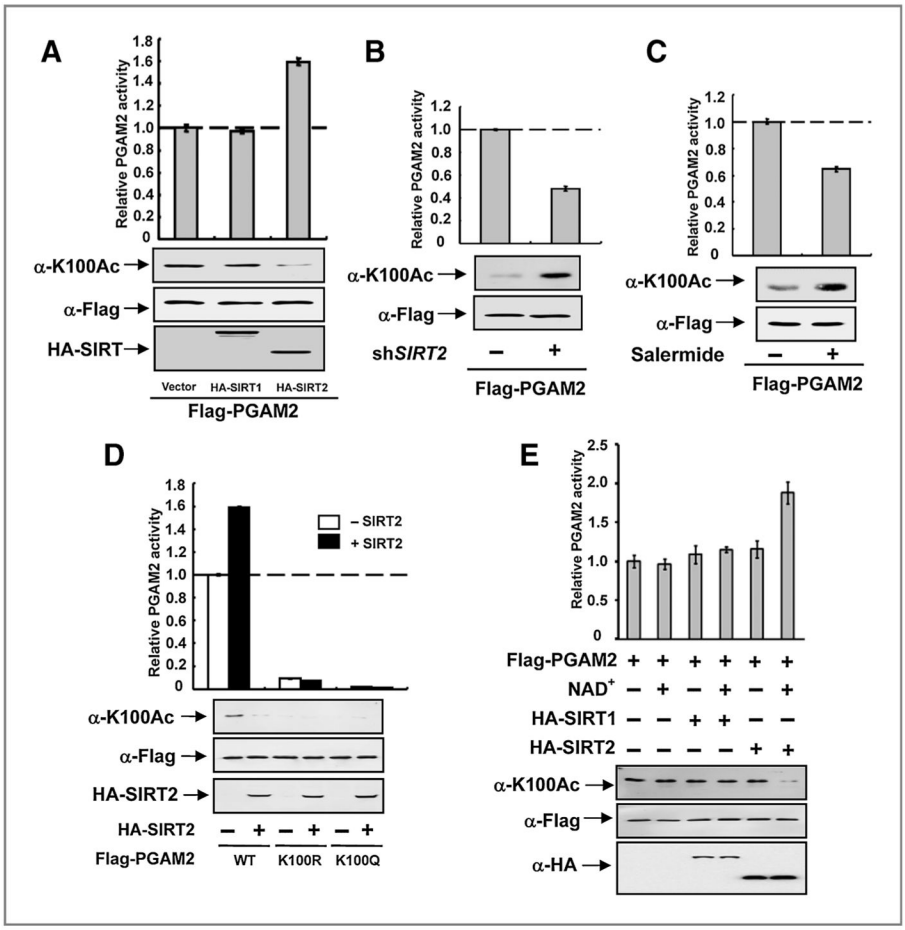

Figure 4.

SIRT2 activates PGAM2. A, SIRT2 increases PGAM2 activity. HEK293T cells were transfected with indicated plasmids, Flag-PGAM2 was immunoprecipitated, and PGAM2 activity was assayed. Mean values of relative enzyme activity of triplicate experiments with ± SD are presented. B, SIRT2 knockdown decreases PGAM2 activity. Scramble and SIRT2 knocking-down stable HEK293T cells were transfected with Flag-PGAM2, and PGAM2 protein was immunoprecipitated and activity was assayed. Error bars represent ± SD for triplicate experiments. C, inhibition of SIRT2 decreases PGAM2 activity. HEK293T cells were transfected with Flag-PGAM2, followed by treatment with salermide. Flag-PGAM2 was immunoprecipitated, and PGAM2 activity was measured. Relative enzyme activities of triplicate experiments ± SD are presented. D, SIRT2 overexpression does not activate K100 mutants of PGAM2. WT and mutant PGAM2 were co-expressed in HEK293T cells with SIRT2, respectively, and purified by Flag beads, followed by enzyme assay and Western blotting. The mean value of triplicates and ± SD are presented. E, SIRT2 deacetylates and activates PGAM2 *in vitro*. Flag-PGAM2, HA-SIRT1, and HA-SIRT2 were purified from HEK293T cells, respectively, and the *in vitro* deacetylation assay was performed as described. Samples were determined by Western blotting with indicated antibodies.

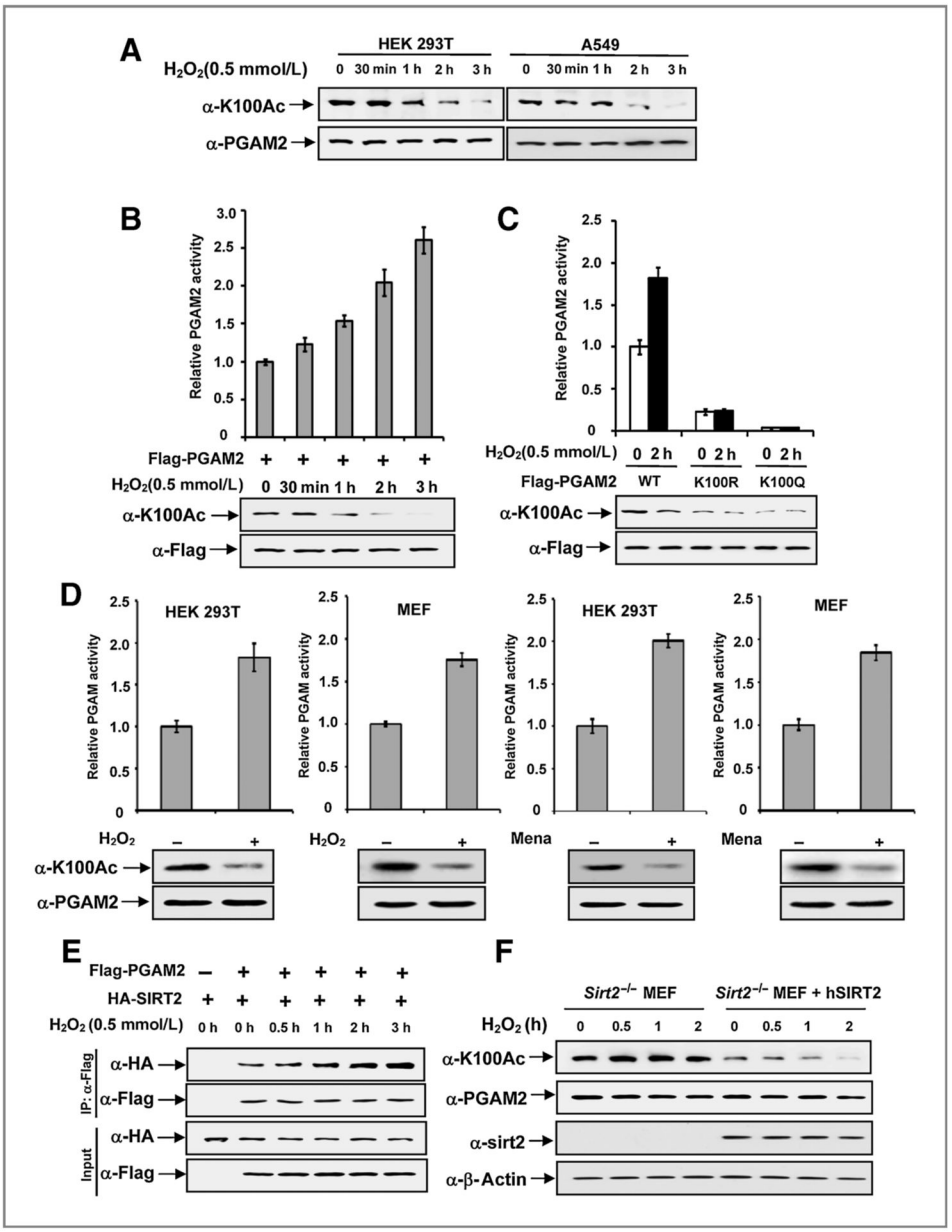

Figure 5.

Oxidative stress decreases K100 acetylation levels and induces PGAM2 activity. A, H_2O_2 treatment decreases endogenous K100 acetylation level. HEK293T and A549 cells were treated with H_2O_2 for different lengths of time as indicated. The levels of K100 acetylation were determined by Western blotting with anti-acetyl-PGAM2 (K100) antibody. B, H_2O_2-induced oxidative stress increases PGAM2 activity. HEK293T cells were transfected with Flag-PGAM2 and then treated with H_2O_2 for indicated time, followed by immunoprecipitation, and enzyme activity was measured and normalized against protein levels. Mean values of relative enzyme activity of triplicate experiments with ± SD are presented. C, H_2O_2 increases WT PGAM2 activity, but not K100 mutants. HEK293T cells were transfected with indicated plasmids, followed by H_2O_2 treatment for 2 hours,

immunoprecipitated, and then PGAM2 activity was assayed. Relative enzyme activities of triplicate experiments ± SD are presented. D, oxidative stress increases the endogenous PGAM activity via reducing the K100 acetylation level. HEK293T cells or WT MEF cells were treated with H_2O_2 for 2 hours or Menadione (Mena) for 30 minutes, respectively, and then endogenous PGAM activity was assayed. The K100 acetylation levels of PGAM2 were determined by Western blot analysis. Relative enzyme activities of triplicate experiments ± SD are presented. E, oxidative stress increases the interaction between SIRT2 and PGAM2. HEK293T cells were transfected with indicated plasmids, and the SIRT2–PGAM2 association was examined by immunoprecipitation (IP)–Western blot analysis. F, Sirt2 mediates K100 deacetylation in response to oxidative stress. *Sirt2*$^{-/-}$ MEFs and *Sirt2*$^{-/-}$ MEFs stably expressing human *SIRT2* were treated with H_2O_2 for indicated time. The change of K100 acetylation levels of PGAM2 was determined by Western blot analysis.

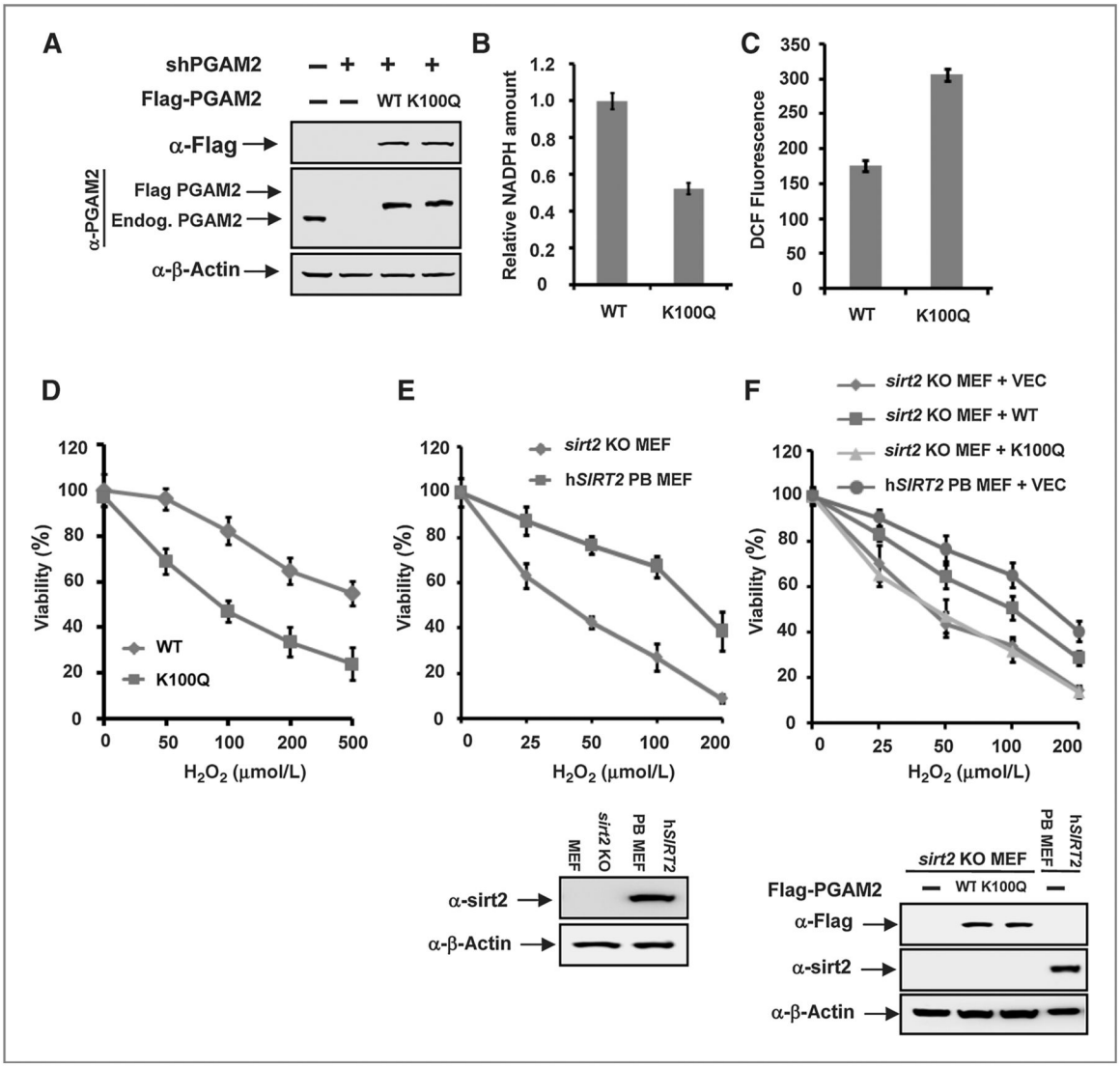

Figure 6.

Acetylation mimetic K100Q mutant reduces NADPH amount and impairs the ability of cells protection from oxidative damage. A, identification of PGAM2 knocking-down and putting-back cell lines. Whole-cell lysates were prepared from PGAM2 knocking-down and putting-back stable cells, PGAM2 knockdown efficiency and re-expression were determined by Western blotting with indicated antibodies. B, A549 cells stably expressing acetylation mimetic K100Q mutant reduces NADPH production. Stable cells identified above were prepared, and NADPH was measured using an NADPH kit. Error bars represent ± SD for triplicate experiments. C, A549 cells expressing acetylation mimetic K100Q mutant accumulates ROS. The same stable cells identified above were prepared, and DCF staining was performed to measure ROS levels. Error bars represent ± SD for triplicate experiments. D, acetylation mimetic K100Q mutant impairs the ability of cells protection from oxidative damage. Stable cells were exposed to different concentrations of H_2O_2 for 24 hours, and the viability of cells was measured by trypan blue exclusion. Error bars represent ± SD for

triplicate experiments. E, *sirt2* KO MEFs are more sensitive to oxidative stress. *sirt2* KO MEFs and human *SIRT2* putting-back (PB) MEFs were exposed to different concentrations of H_2O_2 as indicated for 24 hours, and the viability of cells was measured applying trypan blue exclusion. Error bars represent ± SD for triplicate experiments. F, overexpression of WT PGAM2 in *sirt2* KO MEFs can partially rescue the viability of *sirt2* KO MEFs in response to oxidative stress. Indicated cells were infected with virus expressing PGAM2 wild-type or K100Q mutant for 30 hours, dispersed to 6-well plates, and then exposed to different concentrations of H_2O_2 for 24 hours. The viability of cells was measured by trypan blue exclusion. Error bars represent ± SD for triplicate experiments.

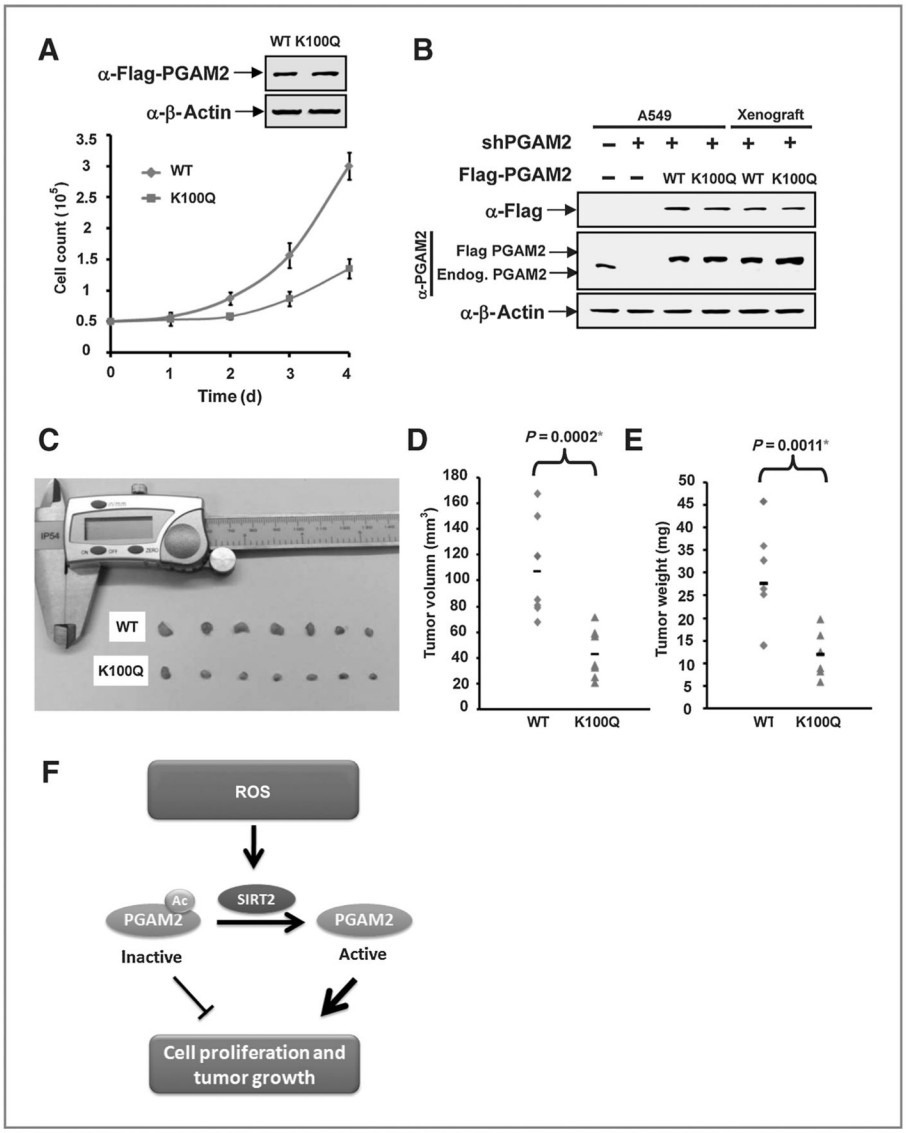

Figure 7.

Acetylation mimetic K100Q mutant inhibits cell proliferation and tumor growth. A, acetylation mimic mutant K100Q suppresses cell proliferation. A total of 5×10^4 indicated stable cells were seeded in each well. Cell numbers were counted every 24 hours. Error bars represent cell numbers ± SD for triplicate experiments. B, the expression of PGAM2 and $PGAM2^{K100Q}$ in stable cell lines and xenograft tumors. Whole-cell extracts were prepared from either original A549 stable cell pools or xenograft tumors, followed analysis by Western blotting. C, acetylation mimic mutant K100Q inhibits xenograft tumor growth *in vivo*. Nude mice were injected with A549 PGAM2 cells or $PGAM2^{K100Q}$ cells. The xenograft tumors were dissected and measured after 7 weeks and shown. D and E, quantification of average volume and weight of xenograft tumors are shown in D and E, respectively. Error bars represent ± SD for 7 tumors.